

Published in final edited form as:

Circ Heart Fail. 2014 March 1; 7(2): 340–350. doi:10.1161/CIRCHEARTFAILURE.113.000984.

Mechanistic Relationship Between MT1-MMP and the Myocardial Response to Pressure-Overload

Michael R. Zile, MD¹, Catalin F. Baicu, PhD¹, Robert E. Stroud, MS², An O. Van Laer, MS¹, Jeffrey A. Jones, PhD², Risha Patel, MS², Rupak Mukherjee, PhD², and Francis G. Spinale, MD, PhD³

¹Division of Cardiology, Department of Medicine, Medical University of South Carolina, and RHJ Department of Veterans Affairs Medical Center, Charleston, SC

²Division of Cardiothoracic Surgery, Department of Surgery, Medical University of South Carolina, and RHJ Department of Veterans Affairs Medical Center, Charleston, SC

³University of South Carolina School of Medicine, and W.J.B. Dorn Department of Veterans Affairs Medical Center, Columbia, SC

Abstract

Background—While matrix metalloproteinases (MMPs) were initially thought to primarily result in extracellular matrix degradation, certain MMP types such as membrane type-1 MMP (MT1-MMP) may also be involved in profibrotic cascades through hydrolysis of latency-associated transforming growth factor (TGF) binding protein (LTBP-1) and activation of TGF dependent profibrotic signaling. The present study tested the hypothesis that MT1-MMP plays a direct role in the matrix remodeling response to a left ventricular (LV) pressure overload (PO) stimulus.

Methods and Results—Wild-type (WT) and transgenic mice with cardiac restricted MT1-MMP over-expression (MT1-OE) or MT1-MMP reduced expression (MT1-RE) underwent PO for 4 weeks. PO resulted in a 57% increase in LV mass (no change in LV end diastolic volume, resulting in an increase in the LV mass / volume ratio consistent with concentric remodeling), a 60% increase in MT1-MMP mediated LTBP-1 hydrolysis, and a 190% increase in collagen content in WT mice. While LV mass was similar between WT, MT1-OE and MT1-RE following PO, significant differences in LV function, MT1-MMP mediated LTBP-1 hydrolysis and collagen content occurred. PO in MT1-OE increased LTBP-1 hydrolysis (18%) collagen content (60%), left atrial dimension (19%; indicative of LV diastolic dysfunction) compared with WT. PO in MT1-RE reduced LAD (19%), LTBP-1 hydrolysis (40%) and collagen content (32%) compared to both WT.

Conclusions—Despite an equivalent PO stimulus and magnitude of LV myocardial growth, altering MT1-MMP levels caused specific matrix dependent changes in remodeling, thereby demonstrating a mechanistic role in the development of the maladaptive remodeling and myocardial fibrotic response to pressure-overload.

Keywords

pressure overload; left ventricular hypertrophy; matrix metalloproteinases

Correspondence to: Michael R. Zile, MD, Division of Cardiology, Department of Medicine, Medical University of South Carolina, Ashley River Towers, 25 Courtenay Drive, Room 7067, Charleston, SC 29425, Telephone: (843) 792-6866, Fax: (843) 789-6850, zilem@musc.edu.

Disclosures
None.

Left ventricular (LV) hypertrophy represents an initial adaptive remodeling response to pressure-overload (PO); however, chronic PO is a progressive process that commonly leads to adverse LV remodeling including the development of myocardial fibrosis and diastolic dysfunction (1–10). Studies that have examined potential causes for this maladaptive response have focused primarily on mechanisms that alter collagen synthesis (8–11). However, there is emerging evidence that suggests that proteolytic events, such as those mediated by matrix metalloproteinases (MMPs), may also contribute to the adverse extracellular matrix (ECM) remodeling that occurs in PO (12–14). For example, our recent studies demonstrated that PO-induced temporal changes in LV structure and function were associated with a time-dependent increase in the induction, expression and abundance of a unique membrane type-1 MMP (MT1-MMP) (1). These findings may appear to contradict the canonical notion that MMP proteolytic activity primarily results in collagen degradation; however, MMPs act on a diverse portfolio of structural proteins and signaling molecules (12, 14, 15). In particular, MT1-MMP may play a critical role in facilitating activation of profibrotic synthetic pathways that result in fibrosis (14). Previous *in vitro* studies showed that MT1-MMP can hydrolyze latency-associated transforming growth factor binding protein (LTBP-1) and release transforming growth factor beta (TGF) (16). TGF is maintained in the ECM in an inactive form through its binding to the LTBPs. LTBP-1 has an MT1-MMP specific hydrolytic site. Once released, TGF undergoes activation, binds to the TGF receptor, activates intracellular signaling pathways that include phosphorylation of SMAD2 (pSMAD), pSMAD2 translocation to the nucleus, and an increase collagen expression (14). Thus, this MT1-MMP-dependent proteolytic activity provides one potential mechanism by which the PO causes activation of profibrotic synthetic pathways that result in fibrosis. Therefore, the purpose of the present study was to directly test the hypothesis that MT1-MMP plays a mechanistic, cause and effect role in the development of the maladaptive remodeling and myocardial fibrotic response to PO. This hypothesis was tested by altering MT1-MMP expression and abundance using transgenic mice that over-express MT1-MMP and transgenic mice with reduced expression of MT1-MMP in a murine model of chronic PO created by transverse aortic constriction.

Methods

Overview and Rationale

To determine whether and to what extent modulation in MT1-MMP abundance alters the myocardial response to pressure-overload, two transgenic mouse lines were created: MT1-MMP over expression (OE) and MT1-MMP reduced expression (RE); FVB wild-type mice (WT) served as controls. Pressure-overload was created in these 3 groups of mice using transverse aortic constriction (PO); mice that did not undergo transverse aortic constriction (non-PO) were also studied in all 3 groups. The experimental response variables were chosen for the following reasons: first, to demonstrate that the transgenic constructs resulted in a change in MT1-MMP activity and a change in MT1-MMP dependent LTBP-1 hydrolytic potential; second, to determine whether changes in MT1-MMP activity resulted in the activation of profibrotic signaling changes in the pSMAD2/SMAD2 ratio and in collagen I A1 and collagen III A1 expression were assessed; third, to determine whether these changes in profibrotic signaling resulted in changes in LV structure, diastolic function, and ECM fibrillar collagen content; and fourth, to determine if these changes in MT1-MMP, LV structure and function altered survival rates.

Transgenic mouse models

Mice with myocardial-restricted expression of human MT1-MMP (MT1-OE) were developed on an FVB background by placing the full-length human gene sequence for MT1-

MMP (GenBank 793762 Accession #90925; 2369bp) under the control of the alpha-myosin heavy chain (α MHC) promoter as previously described (17). The presence of human MT1-MMP was confirmed by RT-PCR using human-specific MT1-MMP primers. A stable, viable colony of this transgenic line was established. Mice born into this colony do not display any phenotypic or developmental abnormalities.

Mice with a global reduction in expression of MT1-MMP (MT1-RE) were developed on an FVB background by replacing exon-4 of the murine MT1-MMP gene sequence with a neomycin cassette by homologous recombination, as previously described (18, 19). The global homozygous MT1-MMP knockout ($-/-$) animals display severe malformation and growth retardation, and typically die around postnatal day 21. The heterozygous offspring, however, have a 50% reduction in MT1-MMP gene copy number, resulting in a ~50% reduction in protein levels. These heterozygous animals have a normal lifespan, do not display any overt phenotypic abnormalities, and produce offspring within the expected Mendelian ratios (1:2:1, +/+, +/-, -/-). Accordingly, heterozygous animals were used for the experiments outlined in this study. Heterozygosity was confirmed by RT-PCR and identified as having the presence of bands for both wild-type MT1-MMP and the neomycin gene upon agarose gel electrophoresis. Fibroblast-specific and cardiomyocyte-specific cardiac-restricted conditional MT1-MMP knockout mice have not yet been created. Whether the homozygous form of these conditional cell specific knockouts would have the same phenotype and limited survival as the global knockout is not known and should be the subject of future investigations.

Pressure Overload

The methods used to create transverse aortic constriction have been previously described (20). All mice were between 12 and 14 weeks of age at the time of PO. Mice were studied 4 weeks following PO. Twenty mice underwent PO in the WT and MT1-RE groups, 40 mice underwent PO in the MT1-OE group. All PO mice had a minimum pressure gradient of 100 mmHg across the transverse aortic constriction. Ten mice did not undergo transverse aortic constriction and served as non-PO controls in each of the 3 groups. In each group discussed above, equal numbers of male and female mice were assigned; thus, 50% of each group was male, 50% were female.

Echocardiography

Echocardiographic measurements were made using a 40 MHz mechanical scanning transducer (707B) and a Vevo 770 echocardiograph (VisualSonics, Inc. Toronto, Canada). LV dimension, volume, wall thickness, ejection fraction (EF), mass, and left atrial dimension (LAD) were measured using the American Society of Echocardiography criteria (21). LV mass was normalized to body weight. LAD was used to reflect chronic changes in LV diastolic pressure; LAD increases as a function of sustained increased LV diastolic pressure (i.e., an integration of pressure over time) (2, 22, 23). The aortic pressure gradient created by PO was measured using the modified Bernoulli equation: Pressure gradient = $4(V_{\text{peak}})^2$, where V_{peak} is the peak Doppler velocity across the transverse aortic constriction (1).

Light Microscopy

Fibrillar collagen content was examined in LV myocardial sections (5 μ m thick) stained with picrosirius red (PSR). A qualitative assessment of collagen content was made from birefringence light microscopy and experimental groups were compared quantitatively based on collagen volume fraction (CVF), defined as the area stained by PSR divided by the total area of interest (20, 24). Fields with large blood vessels were excluded from the analysis.

Areas examined were distributed throughout the myocardium from subendocardial to subepicardial and excluded the epicardial surface.

Cardiomyocyte cross-sectional area (CSA) was measured using previously published techniques in the 6 groups of mice in the current study. Five cells in 10 random fields were measured in each mouse.

MT1-MMP Activity Assays

Myocardial MT1-MMP activity was directly measured in LV myocardium from each mouse using two MT1-MMP specific quenched fluorogenic substrates previously described (25, 26). One substrate, MMP-14 Substrate I (catalog no. 444258, Calbiochem), contained a peptide sequence representing a synthetic MT1-MMP specific cleavage site (17, 25, 27). The second custom designed substrate, SCJJ-1 (AnaSpec), contained a LTBP-1 peptide sequence representing an endogenous MT1-MMP specific hydrolysis site (17, 25). The LV myocardial extracts (50 μ g) were incubated (37°C) in the presence and absence of each MT1-MMP substrate, and excitation/emission were recorded (328/400 nm for the synthetic MT1-MMP peptide, 340/485 nm for the endogenous LTBP-1 peptide FluoStar Galaxy; BMG Labtech) continuously for up to 20 h and compared with a standard curve using active recombinant MT1-MMP (17, 27). Several *in-vitro* validation studies were previously performed in order to demonstrate the specificity of each MT1-MMP substrate (27).

Immunoblot studies for Protein Abundance

SMAD2, and pSMAD2 protein abundance were determined in LV myocardial samples from non-PO or 4-week PO WT, MT1-OE and MT1-RE mice using previously published methods (27). LV samples were thawed and transferred to cold extraction/homogenization buffer [buffer volume: 1:6 (wt/vol)] containing 10 mM cacodylic acid (pH 5.0), 0.15 M NaCl, 10 mM ZnCl₂, 1.5 mM NaN₃, and 0.01% Triton X-100 (vol/vol) and homogenized. Ten micrograms of the supernatant was fractionated on a 4–12% bis-Tris gradient gel. Proteins were transferred to nitrocellulose membranes (0.45 μ m, Bio-Rad) and incubated in antiserum corresponding to total Smad-2, and phosphorylated Smad-2 (#5339 and #3101 respectively, Cell Signaling Technology, Beverly, MA). Antisera was diluted in 5% nonfat dry milk-PBS. A secondary peroxidase-conjugated antibody was then applied (1:5,000, 5% nonfat dry milk-PBS), and signals were detected with a chemiluminescent substrate (Western Lighting Chemiluminescence Reagent Plus, Perkin-Elmer). Band intensity was quantified using Gel-Pro Analyzer software (version 3.1.14, Media Cybernetics, Silver Spring, MD) and reported as the percent change from the non-PO control homogenates.

Gene expression analysis

Changes in collagen I A1 and collagen III A1 expression were examined in all myocardial samples using a RT-PCR method.

RNA Isolation—Myocardial homogenates were subjected to RNA extraction (RNeasy Fibrous Tissue Mini Kit, Qiagen, Valencia, CA), and the quantity and quality of the RNA were determined (Experion Automated Electrophoresis System, Bio-Rad Laboratories, Hercules, CA) using previously published methods (17, 27, 28).

RT-PCR—RNA (1 μ g) was reverse transcribed to generate cDNA (iScript cDNA Synthesis Kit, Bio-Rad). The cDNA was amplified with gene-specific primer/probe sets (TaqMan Universal PCR Master Mix: catalog no. 4364321, Applied Biosystems, Foster City, CA) using single-color RT-PCR (MyiQ, Bio-Rad). The specific primer/probe sets (Applied Biosystems) were collagen I A1 and collagen III A1 (catalog nos. Mm00801666-g1 and Mm01254476-m1). Negative controls were run to verify the absence of genomic DNA

contamination (reverse transcription control), and the absence of overall DNA contamination in the PCR system and working environment (template control). Results from RT-PCR methods are presented as % change from FVB WT non-PO control.

Statistical Analysis

Measurements were analyzed before (non-PO) and 4 weeks after PO in WT, MT1-OE and MT1-RE mice using a two way ANOVA; if significant, pair wise comparisons were made using Tukey's test to adjust for multiple comparisons. Survival curves were constructed using Kaplan–Meier probability estimates and survival at 4 week was compared using a χ^2 analysis. In the current study, only total mortality was examined, cause of death was not examined. The relationships between MT-1 activity, collagen volume fraction and left atrial diameter were assessed using a least squares linear regression analysis. Values of $p < 0.05$ were considered statistically significant. All statistical procedures were performed using the STATA statistical software package (Statacorp, College Station, Tex). Results are presented as mean \pm SEM. Final sample sizes for each protocol/experiment are indicated in Table 1. The authors had full access to the data and take full responsibility for its integrity. All animal procedures were performed in accordance with institutional guidelines.

Results

Survival

Pressure-overload (PO) produced by transverse aortic constriction (TAC) caused a 40% mortality rate in the WT mice, 12 of the 20 assigned to this group survived to the 4 week study point (Figure 1). Modulation of MT1-MMP abundance altered the response to PO. PO in the MT1-OE mice caused an 80% mortality rate (9 of the 40 assigned to this group survived to the 4 week study point) while PO in the MT1-RE mice caused a 20% mortality rate, 16 of the 20 assigned to this group survived to the 4 week study point (Figure 1).

There were no mortalities in the non-PO control mice, all 10 assigned to each group survived to the 4 week study point. WT, MT1OE and MT1-RE mice that did not undergo TAC were followed for 4 weeks, from age 12 weeks to age 16 weeks. There were no mortalities in these 3 non-PO mice (Figure 1).

Structure and Function

Left ventricular structure, systolic function and diastolic function data in the absence of pressure-overload (non-PO) and after 4 weeks of PO in WT, MT1-OE and MT1-RE mice are presented in Table 1. First, the results below will highlight the *effects of pressure-overload* on structure, function and signaling. Second, the results will highlight the effects of *modulation of MT1-MMP abundance* on the response to PO specifically by examining three comparisons: differences between FVB WT PO data (column 2 in Table 1) vs. MT1-OE PO data (column 4), FVB WT PO data (column 2) vs. MT1-RE PO data (column 6), and MT1-OE PO data (column 4) vs. MT1-RE PO data (column 6). All other additional statistical comparisons are presented in Table 1.

Effects of pressure-overload—In WT mice, PO was associated with a 57% increase in LV mass, no change in LV end diastolic volume, and a 79% increase in the LV mass / volume ratio consistent with the development of concentric remodeling (Table 1). In addition, PO was associated with a slightly decreased EF (but EF did not fall below the normal range) and a 59% increase in LAD consistent with the development of diastolic dysfunction (Table 1).

Changes in cardiomyocyte CSA that resulted from PO and transgenic constructs closely paralleled changes in LV mass described above indicating that the level of hypertrophy at the LV chamber level was based on the level of hypertrophy at the cellular level (Table 1).

Effects of modulation of MT1-MMP abundance—At baseline, in the absence of pressure-overload, MT1-OE resulted in small but significant changes in LV structure and function. MT1-OE mice had significantly increased LV mass, no change in LV end diastolic volume, increased LV mass / volume ratio, slightly decreased EF (but still within the normal range), and increased LAD compared to WT mice (Table 1). By contrast, at baseline, in the absence of pressure-overload, MT1-RE resulted in no significant changes in LV structure or function compared to WT mice (Table 1).

After 4 weeks of PO, there were some similarities and some differences in structure and function in the MT1-OE mice compared with the WT mice. After 4 weeks of PO, the LV mass was similar in the MT1-OE mice vs. WT mice. However, because PO caused an increase in LV end diastolic volume in MT1-OE (but not in WT), MT1-OE mice had a smaller LV mass / volume ratio than the WT mice (2.8 ± 0.1 in WT-PO vs. 2.2 ± 0.2 in MT1-OE-PO, $p < 0.001$) (Table 1). In addition, after 4 weeks of PO, EF was 30% lower in the MT1-OE mice vs. WT mice. Finally, after 4 weeks of PO, LAD was 20% higher in the MT1-OE mice vs. WT mice (Table 1).

By contrast, after 4 weeks of PO, LV structure and systolic function in the MT1-RE mice was similar to the WT mice, but both LV diastolic function and survival was less adversely affected in the MT1-RE mice than the WT mice. After 4 weeks of PO, LV mass, LV end diastolic volume, the LV mass / volume ratio and EF were similar in the MT1-RE mice vs. the WT mice (Table 1). In addition, after 4 weeks of PO, LAD was 20% smaller in the MT1-RE mice vs. WT mice (Table 1).

MT1-MMP Dependent Profibrotic Signaling

Effects of pressure-overload—In WT mice, PO was associated with a roughly 60% increase in MT1-MMP activity, LTBP-1 peptide hydrolysis, and the pSMAD-2/SMAD-2 ratio (Figures 2–4).

Effects of modulation of MT1-MMP abundance—At baseline, in the absence of pressure-overload, MT1-OE resulted in an increase in MT1-MMP activity, LTBP-1 peptide hydrolysis, and the pSMAD/SMAD-2 ratio compared to WT mice (Figures 2–4). By contrast, at baseline, in the absence of pressure-overload, MT1-RE mice had a lower MT1-MMP activity, LTBP-1 peptide hydrolysis, and pSMAD-2/SMAD-2 ratio compared to WT mice (Figures 2–4).

After 4 weeks of PO, there was a more robust activation of MT1-MMP dependent profibrotic signaling in MT1-OE mice compared with the WT mice. After 4 weeks of PO, MT1-MMP activity and LTBP-1 peptide hydrolysis were 15% higher in the MT1-OE mice than the WT PO mice (Figures 2 and 3). In addition, after 4 weeks of PO, the pSMAD-2/SMAD-2 ratio was 115% higher in the MT1-OE mice than the WT PO mice (Figure 4). By contrast, after 4 weeks of PO, there was a less robust activation of MT1-MMP dependent profibrotic signaling in MT1-RE mice compared with the WT mice. After 4 weeks of PO, MT1-MMP activity and LTBP-1 peptide hydrolysis were 30% lower in the MT1-RE mice than the WT PO mice (Figures 2 and 3). In addition, after 4 weeks of PO, the pSMAD-2/SMAD-2 ratio was 25% lower in the MT1-RE mice than the WT PO mice (Figure 4).

While changes in both SMAD-2 and pSMAD-2 occurred in these studies, the changes in the ratio were driven primarily by changes in pSMAD-2 (Figure 4).

Collagen Expression and Content

Effects of pressure-overload—In WT mice, PO was associated with a 200% increase in Col1A1 expression, a 130% increase in Col3A1 expression, and a 190% increase in CVF compared to WT PO mice (Figure 5 and 6).

Effects of modulation of MT1-MMP abundance—At baseline, in the absence of pressure-overload, MT1-OE resulted in an increase in Col1A1 and Col3A1 expression and an increase in CVF compared to WT mice (Figure 5 and 6). By contrast, in the absence of pressure-overload, MT1-RE resulted in a slightly lower Col1A1 and Col3A1 expression and a lower CVF compared to WT mice (Figure 5 and 6).

After 4 weeks of PO, collagen expression was a more robust and collagen content was larger in the MT1-OE mice compared with the WT mice. After 4 weeks of PO, Col1A1 expression was 220% higher, Col3A1 expression was 250% higher, and CVF was 30% higher in the MT1-OE mice compared to WT mice (Figure 5 and 6). By contrast, after 4 weeks of PO, collagen expression was a less robust and collagen content was smaller in the MT1-RE mice compared with the WT mice. After 4 weeks of PO, Col1A1 expression was 275% lower, Col3A1 expression was 600% lower, and CVF was 40% lower in the MT1-RE mice compared to WT mice (Figure 5 and 6).

Relationships between MT1-MMP and structural, functional and signaling endpoints

There were direct significant relationships between MT1-MMP activity and left atrial diameter (Figure 7), collagen volume fraction (Figure 7), and the pSMAD2/SMAD2 ratio. In each case as MT1-MMP increased, left atrial diameter ($r=0.62$, $p<0.001$), collagen volume fraction ($r=0.63$, $p<0.001$), and the pSMAD2/SMAD2 ratio ($r=0.52$, $p<0.01$) increased.

Discussion

The current study was designed to define the mechanism by which a specific MMP type, MT1-MMP, directly contributes to the profibrotic response, increased ECM accumulation, and progressive LV diastolic dysfunction that occurs in chronic pressure-overload. Transgenic mice that over-express MT1-MMP or have reduced MT1-MMP expression underwent PO and yielded a number of novel findings that address this fundamental issue. First, PO was associated with MT1-MMP dependent profibrotic signaling; PO caused MT1-MMP induction, increased MT1-MMP activity, MT1-MMP specific LTBP-1 peptide hydrolytic potential, phosphorylation of SMAD-2, collagen expression, collagen content and resulted in diastolic dysfunction. Second, transgenic modulation of MT1-MMP abundance fundamentally changed this PO-induced MT1-MMP dependent profibrotic signaling response but did not change the magnitude of the hypertrophic response to PO. MT1-MMP over-expression markedly increased profibrotic signaling; MT1-MMP reduced expression significantly decreased profibrotic signaling; but neither directional modulation of MT1-MMP altered the extent of PO-induced hypertrophy. Thus, the induction of a unique transmembrane proteolytic enzyme provides a fundamental mechanism that influences the myocardial response to PO. Specifically, there is a mechanistic relationship between the changes in MT1-MMP abundance and changes in ECM structure and LV diastolic function that occur during PO. In addition to these and other data underscoring the fact that MMPs have a diversity of both function and substrates, these data provide insight into the specific molecular pathways by which MT1-MMP induction contributes to the ECM remodeling and fibrosis that represent one critical event that occurs during the progression from chronic PO to diastolic dysfunction.

Mechanisms of Diastolic Dysfunction: Cellular vs. Extracellular Mechanisms

Abnormalities in diastolic function are consequent to changes in both the cardiomyocyte and the ECM (15, 29–31). Cardiomyocyte abnormalities occur largely in the context of the development of LV hypertrophic growth. PO-induced increase in LV mass and cardiomyocyte hypertrophy have been thought to constitute an initial adaptive mechanism that normalizes or limits the increase in LV systolic wall stress that occurs in PO (32). However, progressive hypertrophy may become maladaptive and result in diastolic dysfunction (1). Unlike cardiomyocyte hypertrophy, ECM fibrosis is always maladaptive and results in diastolic dysfunction (8). These facts add to the complexity of defining which cellular and molecular mechanisms represent the causal mechanisms responsible for diastolic dysfunction in PO. Fortunately, modulation of MT1-MMP expression in the context of the current study did not alter the hypertrophic response to PO, but selectively affected the ECM remodeling response to PO. Thus, MT1-MMP dependent ECM remodeling represents an independent mechanism causing diastolic dysfunction. In the current study, the extent of diastolic dysfunction was assessed by examining changes in left atrial size. Left atrial size serves to integrate the increase in LV diastolic pressure over time. There were direct relationships between MT1-MMP activity and left atrial diameter, collagen volume fraction and mortality. As MT1-MMP increased, left atrial diameter, collagen volume fraction, and mortality increased; the converse occurred when MT1-MMP abundance fell. Furthermore, the PO-induced diastolic dysfunction appears to be related to activation of a TGF-dependent profibrotic signaling pathway. These data are concordant with human and animal studies that suggested that TGF-dependent profibrotic signaling is a consistent finding in chronic pressure-overload (3–38). In addition, the current study identified MT1-MMP as a critical factor in the activation of this signaling pathway beginning with MT1-MMP dependent LTBP-1 proteolysis, TGF release, SMAD phosphorylation, and increased collagen synthesis.

MMP-induced Proteolytic vs. Profibrotic Signaling

Data suggest that the pathways by which MT1-MMP contribute to adverse ECM remodeling likely include facilitating localized proteolysis of interstitial molecules directly (such as integrins) causing remodeling, amplification of active soluble MMPs (such as MMP-2) causing ECM instability and abnormal architecture, as well as through enhancing profibrotic signaling pathways (such as TGF- β) causing fibrosis (39–45). TGF- β is maintained in the ECM in an inactive form through its binding to the latent TGF binding protein-1 (LTBP). LTBP-1 has an MT1-MMP specific hydrolytic site. Through a number of *in-vitro* and proteolytic assays, it has been demonstrated that MT1-MMP processes LTBP-1, which releases TGF- β (14, 46–48). Once released, TGF- β undergoes activation, binds to the TGF receptor, activates intracellular signaling pathways that include phosphorylation of SMAD2 (pSMAD). pSMAD2 translocates to the nucleus, regulates transcription in a profibrotic manner including an increase collagen expression (37, 38). The TGF signaling pathway is complex, involves a number of different transmembrane receptors, a number of different SMAD proteins, and has both canonical and non-canonical components including TGF- β /TAK1/p-38 MAPK pathway that play an important role in the maladaptive hypertrophy and dysfunction that develops with PO (49). It was beyond the purpose of this study to examine all of these components of TGF signaling pathway; however, data presented in the current study does indicate that PO activates a TGF associated signaling pathway that is modulated by, if not actually initiated by MT1-MMP. Transgenic modulation of MT1-MMP altered these profibrotic signaling pathways; increased MT1-MMP increasing, decreased MT1-MMP decreasing TGF signaling.

MT1-MMP in Adverse Myocardial Remodeling

Previous studies have shown that the specific pattern of ECM remodeling and the functional changes that result from this remodeling are critically dependent on the type of hemodynamic overload present (14, 15, 32). The cellular and molecular mechanisms responsible for these differences in ECM remodeling have not been completely defined. The current study and previous studies have attempted to define a differential pattern of selective MMP induction in pressure vs. volume-overload (14, 15). The volume overload that follows a myocardial infarction leads to eccentric remodeling and increased expression and activity of MT1-MMP. Because the LV remodeling is distinctly different in pressure-overload compared with volume-overload, there is no a priori reason to believe that the MT1-MMP/LTBP-1/TGF- β /SMAD signaling pathway would be activated in pressure-overload, at least not in the same fashion. However, data from the current study showed that the induction of MT1-MMP occurs in both volume and pressure-overload (14, 15). How do these different pathologic stimuli lead to an increase in MT1-MMP and how does an increase in MT1-MMP play a cause and effect role in each form of LV remodeling? While the current study does not address the entirety of this question, it does provide significant new insight into a number of possible answers. The different biophysical stimuli created in pressure vs. volume-overload result in an individualized portfolio of context specific substrates. MT1-MMPs effect on these stimulus-dependent, context-specific, but different substrates results in distinctly different effects on collagen homeostasis and changes in LV structure and function.

For example, volume-overload causes significant increases in LV diastolic volume and end diastolic wall stress with less pronounced changes in end systolic wall stress. *In vivo* and *in vitro* studies have shown that these changes in mechanical load are sufficient to increase MT1-MMP, MMP-2 (and other soluble MMPs), and a host of inflammatory cytokines (such as TNF) (1, 14, 15). In addition, volume-overload generally decreases the tissue inhibitors of MMP (TIMPs) (14, 15). Context specific substrates such as MMP-2 and TNF and its downstream proteolytic cascade are the principle targets of MT1-MMP that result in ECM proteolysis, LV dilation, eccentric remodeling, and systolic dysfunction. These proteolytic effects are not limited by increased TIMPs. By contrast, pressure-overload causes significant increases in end systolic wall stress with less pronounced changes in end diastolic wall stress (32). These changes in mechanical load lead to increased MT1-MMP but also a significant increase in TIMPs which act to limit ECM proteolysis (1, 14, 15). The MT1-MMP dependent activation of MMP-2 that occurs with PO acts in a concert complex between MMP-2, MT1-MMP and TIMP-2 to hydrolyse LTBP-1. Thus, PO-induced MT1-MMP induction acts on the context specific substrate LTBP-1, leading to activation of TGF, and the TGF-dependent profibrotic signaling process. Therefore, differences in biophysical stimuli result in an individualized portfolio of context specific substrates that allows MT1-MMP to serve as a common mechanism for differential LV remodeling. In addition to profibrotic signaling induced LV remodeling, selective changes in MMPs, TIMPs, and TGF may induce other pleiotropic effects such as inflammation, angiogenesis, and apoptosis/autophagy that may affect LV structural and functional remodeling in response to hemodynamic load.

Other ECM Regulatory Mechanisms

The current study focused specifically on ECM regulatory mechanisms effecting collagen synthesis. However, it is recognized that in addition to synthesis, mechanisms regulating collagen post-synthetic processing, and collagen degradation also determine ECM collagen structure, geometry and content (1, 8, 14, 15, 20). For example, PO has been shown to increase TIMPs which may act to limit the effects of MMPs and therefore decrease collagen degradation (14, 15, 50). There is no a priori reason to expect that transgenic MT1-MMP

modulation will alter TIMP expression. In addition, TIMPs have poor affinity for MT1-MMP but have a uniformly high affinity for soluble MMPs. Therefore, TIMPs provide potent inhibition to soluble MMPs, but do not significantly modify MT1-MMP activity (51, 52). Thus, the aggregate effects of PO-induced increased MT1-MMP activity (not blunted by TIMPs) acting on context specific substrates such as LTBP-1 and activating downstream TGF profibrotic cascade result in myocardial fibrosis.

Future Directions

Using transgenic constructs provides the advantage of being able to increase or decrease the expression of a single gene product; in the current experiment this was specific to MT1-MMP. However, this change in MT1-MMP expression is life long and may result in unintended secondary changes. In addition, the creation of a PO can only be performed in the presence of a permanent condition of increased or decreased MT1-MMP expression. Thus, the change in MT1-MMP expression cannot be limited to only a period during which PO is induced and cannot be changed after PO is complete. Future studies should be designed to address these limitations using a conditional transgenic mouse model in which an inducible construct can be studied. Alternatively, a systemically applied selective inhibitor of MT1-MMP might be used.

In the murine models used in the current study, there are significant limitations in the ability to determine the cause of death and in performing sufficient surveillance to predict cause and occurrence of mortality. Defining cause of death in murine models is exceedingly difficult. Post mortem examinations are often ambiguous. For example, even when post mortem findings of pericardial and pleural effusion suggests increased LV diastolic filling pressures, primary arrhythmic death may have occurred blurring the distinction between death caused by heart failure versus arrhythmia. Therefore, the cause of death was not formally investigated in this study. However, the time course of changes in LV structure and function that results from pressure-overload induced by transverse aortic constriction was carefully defined in a recent study (1). In this study, mice underwent echocardiographic studies at 1, 2 or 4 weeks after PO; at each time point mice underwent terminal studies, thus serial studies in each individual mouse was not performed. In addition, structural and functional changes measured at 5–7 days after PO have not been shown to predict mortality rates or mode of death in this murine model. Therefore, serial imaging studies were not performed in the transgenic mice used in the current study. This is clearly an important area for future studies.

Clinical Implications

The transition from PO-induced remodeling to diastolic dysfunction and myocardial fibrosis represents a pivotal development in the clinical course of hypertensive heart disease (HHD) and HFpEF. Management strategies for patients with HHD and HFpEF represent a large unmet need and require new directions that target underlying pathophysiologic mechanisms. Our studies show that the murine model of transverse aortic constriction-induced PO causes changes in LV structure and function that are similar to the structure-function changes in HHD and HFpEF. Therefore, the MT1-MMP-dependent changes in profibrotic signaling represent a clinically relevant causal mechanism that may serve as potential therapeutic targets to prevent or reverse PO-induced adverse ECM remodeling. For example, data from the current study suggest that a decrease in MT1-MMP induction, rather than a complete ablation of MT1-MMP may be sufficient to modify ECM remodeling in PO. Because MT1-MMP is processed intracellularly by a furin dependent mechanism and released onto the cell surface as a pre-activated MMP form, furin inhibitors, currently being developed for oncologic application, may hold promise for patients with HHD and HFpEF (53). Future basic and translational studies should target these therapeutic applications.

Conclusions

Pressure-overload induction of a unique transmembrane proteolytic enzyme provides a fundamental mechanism influencing the myocardial response to pressure-overload. Variations in MT1-MMP did not lead to alterations in the induction of the hypertrophic response to increased stress; however, PO induced MT1-MMP-dependent profibrotic signaling lead to alterations in interstitial fibrosis and diastolic function. Thus, these data suggest that there is a direct mechanistic relationship between the changes in MT1-MMP and changes in ECM structure and LV diastolic function that occur during pressure-overload.

Supplementary Material

Refer to Web version on PubMed Central for supplementary material.

Acknowledgments

Sources of Funding

This work was supported by the National Institute of Health grants HL057952, HL089944, HL095608, and Merit Awards from the Veterans' Affairs Health Administration. Drs. Michael Zile and Francis Spinale are supported by the Research Service of the Department of Veterans Affairs. Dr. Michael Zile is supported by the Research Service of the Department of Veterans Affairs (5101CX000415-02 and 5101BX000487-04).

References

1. Zile MR, Baicu CF, Stroud RE, Van Laer A, Arroyo J, Mukherjee R, Jones JR, Spinale FG. Pressure-Overload Department Membrane-Type 1 Matrix Metalloproteinase Induction: Relationship to LV Remodeling and Fibrosis. *Am J Physiol Heart Circ Physiol*. 2012; 302:H1429–437. [PubMed: 22287584]
2. Zile MR, Gottdiener JS, Hetzel SJ, McMurray JJ, Komajda M, McKelvie R, Baicu CF, Massie BM, Carson PE. Prevalence and Significance of Alterations in Cardiac Structure and Function in Patients with Heart Failure and a Preserved Ejection Fraction. *Circulation*. 2011; 124:2491–2501. [PubMed: 22064591]
3. Zile MR, Baicu CF, Gaasch WH. Diastolic heart failure—abnormalities in active relaxation and passive stiffness of the left ventricle. *N Engl J Med*. 2004; 350:1953–1959. [PubMed: 15128895]
4. Westermann D, Kasner M, Steendijk P, Spillmann F, Riad A, Weitmann K, Hoffmann W, Poller W, Pauschinger M, Schultheiss HP, Tschöpe C. Role of Left Ventricular Stiffness in Heart Failure With Normal Ejection Fraction. *Circulation*. 2008; 117:2051–2060. [PubMed: 18413502]
5. Weidemann F, Herrmann S, Störk S, Niemann M, Frantz S, Lange V, Beer M, Gattenlöhner S, Voelker W, Ertl G, Strotmann JM. Impact of myocardial fibrosis in patients with symptomatic severe aortic stenosis. *Circulation*. 2009; 120:577–584. [PubMed: 19652094]
6. Azevedo CF, Nigri M, Higuchi ML, Pomerantzeff PM, Spina GS, Sampaio RO, Tarasoutchi F, Grinberg M, Rochitte CE. Prognostic significance of myocardial fibrosis quantification by histopathology and magnetic resonance imaging in patients with severe aortic valve disease. *J Am Coll Cardiol*. 2010; 56:278–287. [PubMed: 20633819]
7. Kasner M, Westermann D, Lopez B, Gaub R, Escher F, Kühl U, Schultheiss HP, Tschöpe C. Diastolic tissue Doppler indexes correlate with the degree of collagen expression and cross-linking in heart failure and normal ejection fraction. *J Am Coll Cardiol*. 2011; 57:977–985. [PubMed: 21329845]
8. Baicu CF, Li J, Zhang Y, Kasiganesan H, Cooper G, Zile MR, Bradshaw AD. Time Course of Right Ventricular Pressure-Overload Induced Myocardial Fibrosis: Relationship to Changes in Fibroblast Dependent Post-synthetic Procollagen Processing. *Am J Physiol Heart Circ Physiol*. 2012; 303:H1128–1134. [PubMed: 22942178]
9. Spinale FG. Myocardial matrix remodeling and the matrix metalloproteinases: influence on cardiac form and function. *Physiol Rev*. 2007; 87:1285–1342. [PubMed: 17928585]

10. Creemers EE, Pinto YM. Molecular mechanisms that control interstitial fibrosis in the pressure-overloaded heart. *Cardiovasc Res.* 2011; 89:265–272. [PubMed: 20880837]
11. Goldsmith EC, Bradshaw AD, Spinale FG. Cellular mechanisms of tissue fibrosis. 2. Contributory pathways leading to myocardial fibrosis: moving beyond collagen expression. *Am J Physiol Cell Physiol.* 2013; 304:C393–402. [PubMed: 23174564]
12. Iyer RP, Patterson NL, Fields GB, Lindsey ML. The history of matrix metalloproteinases: milestones, myths, and misperceptions. *Am J Physiol Heart Circ Physiol.* 2012; 303:H919–930. [PubMed: 22904159]
13. Malesmud CJ. Matrix metalloproteinases (MMPs) in health and disease: an overview. *Front Biosci.* 2006; 11:1696–1701. [PubMed: 16368548]
14. Spinale FG, Janicki JS, Zile MR. Membrane Associated Matrix Proteolysis and Heart Failure. *Circ Res.* 2013; 112:195–208. [PubMed: 23287455]
15. Spinale FG, Zile MR. Integrating the Myocardial Matrix into Heart Failure Recognition and Management. *Circ Res.* 2013; 113:725–38. [PubMed: 23989715]
16. Karsdal MA, Larsen L, Engsig MT, Lou H, Ferreras M, Lochter A, Delaisse JM, Foged NT. Matrix metalloproteinase-dependent activation of latent transforming growth factor-beta controls the conversion of osteoblasts into osteocytes by blocking osteoblast apoptosis. *J Biol Chem.* 2002; 277:44061–44067. [PubMed: 12226090]
17. Spinale FG, Escobar GP, Mukherjee R, Zavadzkas JA, Saunders SM, Jeffords LB, Leone AM, Beck C, Bouges S, Stroud RE. Cardiac-restricted overexpression of membrane type-1 matrix metalloproteinase in mice: effects on myocardial remodeling with aging. *Circ Heart Fail.* 2009; 2:351–360. [PubMed: 19808359]
18. Zhou Z, Apte SS, Soininen R, Cao R, Baaklini GY, Rauser RW, Wang J, Cao Y, Tryggvason K. Impaired endochondral ossification and angiogenesis in mice deficient in membrane-type matrix metalloproteinase 1. *Proc Natl Acad Sci USA.* 2000; 97:4052–4057. [PubMed: 10737763]
19. Zavadzkas JA, Mukherjee R, Rivers WT, Patel RK, Meyer EC, Black LE, McKinney RA, Oelsen JM, Stroud RE, Spinale FG. Direct regulation of membrane type 1 matrix metalloproteinase following myocardial infarction causes changes in survival, cardiac function, and remodeling. *Am J Physiol Heart Circ Physiol.* 2011; 301:H1656–1666. [PubMed: 21666120]
20. Bradshaw AD, Baicu CF, Rentz TJ, Van Laer AO, Boggs J, Lacy JM, Zile MR. Pressure overload-induced alterations in fibrillar collagen content and myocardial diastolic function: role of secreted protein acidic and rich in cysteine (SPARC) in post-synthetic procollagen processing. *Circulation.* 2009; 119:269–280. [PubMed: 19118257]
21. Lang RM, Bierig M, Devereux RB, Flachskampf FA, Foster E, Pellikka PA, Picard MH, Roman MJ, Seward J, Shanewise JS, Solomon SD, Spencer KT, John Sutton M, Stewart WJ. Recommendations for Chamber Quantification: A Report from the American Society of Echocardiography’s Guidelines and Standards Committee and the Chamber Quantification Writing Group, Developed in Conjunction with the European Association of Echocardiography, a Branch of the European Society of Cardiology. *J Am Soc Echocardiogr.* 2005; 18:1440–1463. [PubMed: 16376782]
22. Lam CS, Roger VL, Rodeheffer RJ, Bursi F, Borlaug BA, Ommen SR, Kass DA, Redfield MM. Cardiac structure and ventricular-vascular function in persons with heart failure and preserved ejection fraction from Olmsted County, Minnesota. *Circulation.* 2007; 115:1982–1990. [PubMed: 17404159]
23. Melenovsky V, Borlaug BA, Rosen B, Hay I, Ferruci L, Morell CH, Lakatta EG, Najjar SS, Kass DA. Cardiovascular features of heart failure with preserved ejection fraction versus nonfailing hypertensive left ventricular hypertrophy in the urban Baltimore community: the role of atrial remodeling/dysfunction. *J Am Coll Cardiol.* 2007; 49:198–207. [PubMed: 17222731]
24. Blom AS, Mukherjee R, Pilla JJ, Lowry AS, Yarbrough WM, Mingoia JT, Hendrick JW, Stroud RE, McLean JE, Affuso J, Gorman RC, Gorman JH 3rd, Acker MA, Spinale FG. Cardiac support device modifies left ventricular geometry and myocardial structure after myocardial infarction. *Circulation.* 2005; 112:1274–1283. [PubMed: 16129812]
25. Deschamps AM, Yarbrough WM, Squires CE, Allen RA, McClister DM, Dowdy KB, McLean JE, Mingoia JT, Sample JA, Mukherjee R, Spinale FG. Trafficking of the membrane type-1 matrix

- metalloproteinase in ischemia and reperfusion: relation to interstitial membrane type-1 matrix metalloproteinase activity. *Circulation*. 2005; 111:1166–1174. [PubMed: 15723986]
26. Dixon JA, Gaillard WF 2nd, Rivers WT, Koval CN, Stroud RE, Mukherjee R, Spinale FG. Heterogeneity in MT1-MMP activity with ischemia-reperfusion and previous myocardial infarction: relation to regional myocardial function. *Am J Physiol Heart Circ Physiol*. 2010; 299:H1947–1958. [PubMed: 20935147]
 27. Spinale FG, Mukherjee R, Zavadzka JA, Koval CN, Bouges S, Stroud RE, Dobrucki LW, Sinusas AJ. Cardiac restricted overexpression of membrane type-1 matrix metalloproteinase causes adverse myocardial remodeling following myocardial infarction. *J Biol Chem*. 2010; 285:30316–30327. [PubMed: 20643648]
 28. Ruddy JM, Jones JA, Stroud RE, Mukherjee R, Spinale FG, Ikonomidis JS. Differential effects of mechanical and biological stimuli on matrix metalloproteinase promoter activation in the thoracic aorta. *Circulation*. 2009; 120:S262–268. [PubMed: 19752377]
 29. van Heerebeek L, Franssen CP, Hamdani N, Verheugt FW, Somsen GA, Paulus WJ. Curr. Molecular and Cellular Basis for Diastolic Dysfunction. *Curr Heart Fail Rep*. 2012; 9:293–302. [PubMed: 22926993]
 30. Hamdani N, Paulus WJ. Myocardial titin and collagen in cardiac diastolic dysfunction: partners in crime. *Circulation*. 2013; 128:5–8. [PubMed: 23709670]
 31. Zile MR.; Baicu, CF. Alterations in Ventricular Function: Diastolic Heart Failure. In: Mann, DL., editor. *Heart Failure: A Companion to Braunwald's Heart Disease*. 2. Vol. Chapter 14. Elsevier; Philadelphia, PA: 2010.
 32. Gaasch WH, Zile MR. Left Ventricular Structural Remodeling In Health And Disease: With Special Emphasis on Volume, Mass, and Geometry. *J Am Coll Cardiol*. 2011; 58:1733–1740. [PubMed: 21996383]
 33. Villar AV, García R, Llano M, Cobo M, Merino D, Lantero A, Tramullas M, Hurlé JM, Hurlé MA, Nistal JF. BAMB1 (BMP and activin membrane-bound inhibitor) protects the murine heart from pressure-overload biomechanical stress by restraining TGF- β signaling. *Biochim Biophys Acta*. 2013; 1832:323–335. [PubMed: 23168040]
 34. Dobaczewski M, Chen W, Frangogiannis NG. Transforming growth factor (TGF)-beta signaling in cardiac remodeling. *J Mol Cell Cardiol*. 2011; 51:600–606. [PubMed: 21059352]
 35. Villar AV, Cobo M, Llano M, Montalvo C, Gonzalez-Vilchez F, Martin-Duran R, Hurlé MA, Nistal JF. Plasma levels of transforming growth factor-beta 1 reflect left ventricular remodeling in aortic stenosis. *PLoS One*. 2009; 4:e8476. [PubMed: 20041033]
 36. Gordon KJ, Blobe GC. Role of transforming growth factor- β superfamily signaling pathways in human disease. *Biochim Biophys Acta*. 2008; 1782:197–228. [PubMed: 18313409]
 37. Bjornstad JL, Skrbic B, Marstein HS, Hasic A, Sjaastad I, Louch WE, Florholmen G, Christensen G, Tonnessen T. Inhibition of SMAD2 phosphorylation preserves cardiac function during pressure overload. *Cardiovasc Res*. 2012; 93:100–110. [PubMed: 22049534]
 38. Bujak M, Ren G, Kweon HJ, Dobaczewski M, Reddy A, Taffet G, Wang XF, Frangogiannis NG. Essential role of smad3 in infarct healing and in the pathogenesis of cardiac remodeling. *Circulation*. 2007; 116:2127–2138. [PubMed: 17967775]
 39. Koshikawa N, Minegishi T, Sharabi A, Quaranta V, Seiki M. Membrane-type matrix metalloproteinase-1 (MT1-MMP) is a processing enzyme for human laminin gamma 2 chain. *J Biol Chem*. 2005; 280:88–93. [PubMed: 15525652]
 40. Kridel SJ, Sawai H, Ratnikov BI, Chen EI, Li W, Godzik A, Strongin AY, Smith JW. A unique substrate binding mode discriminates membrane type-1 matrix metalloproteinase from other matrix metalloproteinases. *J Biol Chem*. 2002; 277:23788–23793. [PubMed: 11959855]
 41. Kudo T, Takino T, Miyamori H, Thompson EW, Sato H. Substrate choice of membrane-type 1 matrix metalloproteinase is dictated by tissue inhibitor of metalloproteinase-2 levels. *Cancer Sci*. 2007; 98:563–568. [PubMed: 17425593]
 42. Newby AC. Matrix metalloproteinases regulate migration, proliferation, and death of vascular smooth muscle cells by degrading matrix and non-matrix substrates. *Cardiovasc Res*. 2006; 69:614–624. [PubMed: 16266693]

43. Ohuchi E, Imai K, Fujii Y, Sato H, Seiki M, Okada Y. Membrane type 1 matrix metalloproteinase digests interstitial collagens and other extracellular matrix macromolecules. *J Biol Chem.* 1997; 272:2446–51. [PubMed: 8999957]
44. Williams LM, Gibbons DL, Gearing A, Maini RN, Feldmann M, Brennan FM. Paradoxical effects of a synthetic metalloproteinase inhibitor that blocks both p55 and p75 TNF receptor shedding and TNF alpha processing in RA synovial membrane cell cultures. *J Clin Invest.* 1996; 97:2833–2841. [PubMed: 8675695]
45. Guo C, Piacentini L. Type I Collagen-induced MMP-2 Activation Coincides with Up-regulation of Membrane Type 1-Matrix Metalloproteinase and TIMP-2 in Cardiac Fibroblasts. *J Biol Chem.* 2003; 278:46699–46708. [PubMed: 12970340]
46. Dallas SL, Rosser JL, Mundy GR, Bonewald LF. Proteolysis of latent transforming growth factor-beta (TGF-beta)-binding protein-1 by osteoclasts. A cellular mechanism for release of TGF-beta from bone matrix. *J Biol Chem.* 2002; 277:21352–21360. [PubMed: 11929865]
47. Tatti O, Vehviläinen P, Lehti K, Keski-Oja J. MT1-MMP releases latent TGF-beta1 from endothelial cell extracellular matrix via proteolytic processing of LTBP-1. *Exp Cell Res.* 2008; 314:2501–2514. [PubMed: 18602101]
48. Hawinkels LJ, Kuiper P, Wiercinska E, Verspaget HW, Liu Z, Pardali E, Sier CF, ten Dijke P. Matrix metalloproteinase-14 (MT1-MMP)-mediated endoglin shedding inhibits tumor angiogenesis. *Cancer Res.* 2010; 70:4141–4150. [PubMed: 20424116]
49. Koitabashi N, Danner T, Zaiman AL, Pinto YM, Rowell J, Mankowski J, Zhang D, Nakamura T, Takimoto E, Kass DA. Pivotal role of cardiomyocyte TGF-beta signaling in the murine pathological response to sustained pressure overload. *J Clin Invest.* 2011; 121:2301–12. [PubMed: 21537080]
50. Polyakova V, Hein S, Kostin S, Ziegelhoeffer T, Schaper JJ. Matrix metalloproteinases and their tissue inhibitors in pressure-overloaded human myocardium during heart failure progression. *Am Coll Cardiol.* 2004; 44:1609–1618.
51. Zhao H, Bernardo MM, Osenkowski P, Sohail A, Pei D, Nagase H, Kashiwagi M, Soloway PD, DeClerck YA, Fridman R. Differential inhibition of membrane type 3 (MT3)-matrix metalloproteinase (MMP) and MT1-MMP by tissue inhibitor of metalloproteinase (TIMP)-2 and TIMP-3 regulates pro-MMP-2 activation. *J Biol Chem.* 2004; 279:8592–601. [PubMed: 14681236]
52. Gomez DE, Alonso DF, Yoshiji H, Thorgeirsson UP. Tissue inhibitors of metalloproteinases: structure, regulation and biological functions. *Eur J Cell Biol.* 1997; 74:111–22. [PubMed: 9352216]
53. Coppola JM, Bhojani MS, Ross BD, Rehemtulla A. A small-molecule furin inhibitor inhibits cancer cell motility and invasiveness. *Neoplasia.* 2008; 10:363–370. [PubMed: 18392131]

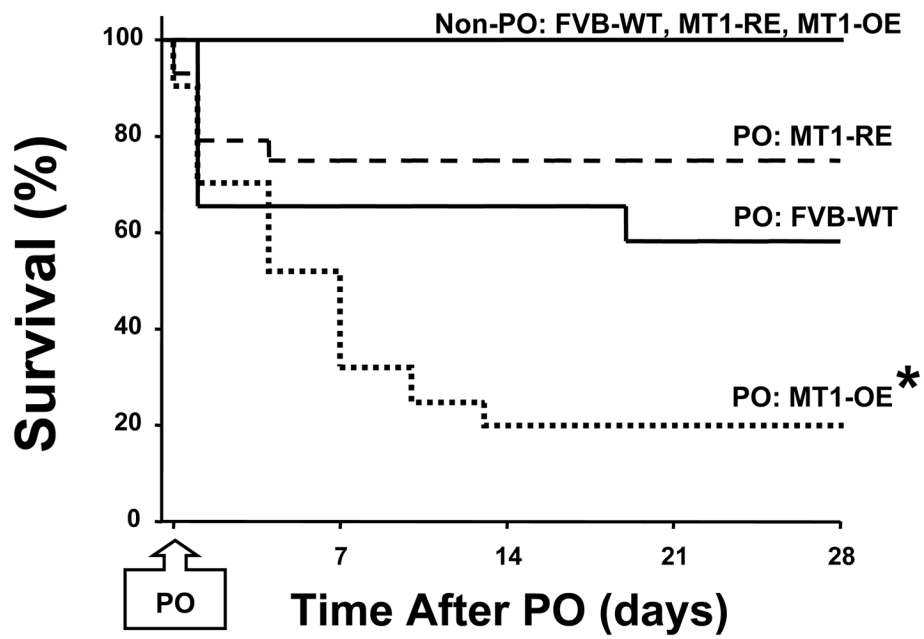


Figure 1. Effects of chronic pressure-overload (PO) on survival in FVB wild-type (WT) versus membrane type one matrix metalloproteinase (MT1-MMP) over-expression (OE) versus MT1-MMP reduced expression (RE) mice. There was a markedly decreased survival rate in the MT1-OE mice (from 40 to 9) compared with WT mice (from 20 to 12) but a small increase in survival in the MT1-RE mice (from 20 to 16). * = $p < 0.05$ vs. FVB Wild-Type. Non-PO = mice that did not undergo transverse aortic constriction (10 in each group).

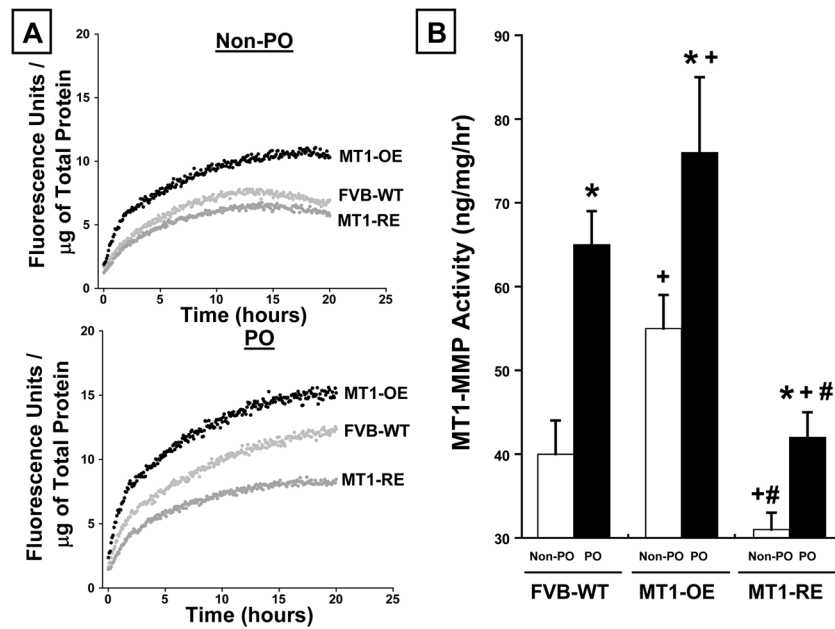


Figure 2. Chronic pressure-overload (PO) induced changes in membrane type one matrix metalloproteinase (MT1-MMP) activity. Panel A: Representative examples and Panel B: mean data in FVB wild-type (WT, n = 10 non-PO, 12 PO) versus MT1-MMP over-expression (OE, n = 10 non-PO, 9 PO) versus MT1-MMP reduced expression (RE, n = 10 non-PO, 16 PO) mice. MT1-OE mice had an increase in MT1-MMP activity and abundance before (non-PO) and after PO compared with WT mice. By contrast, the MT1-RE mice had a significantly lower MT1-MMP activity and abundance before PO and a significantly blunted increase in MT1-MMP activity and abundance after PO compared with both WT and MT1-OE mice. * = $p < 0.05$ vs. strain matched non PO control, + = $p < 0.05$ vs. conditioned matched FVB WT, # = $p < 0.05$ vs. conditioned matched MT1-OE.

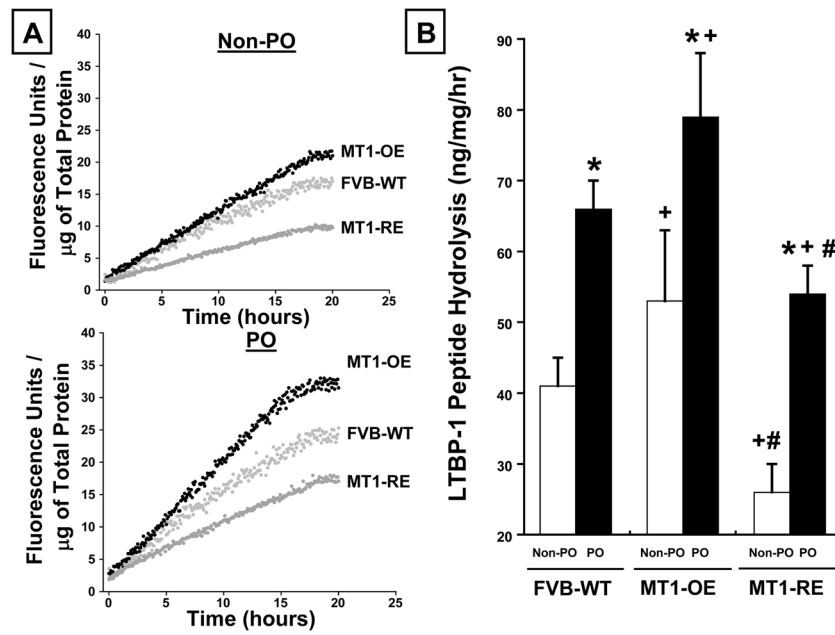


Figure 3. Chronic pressure-overload (PO) induced changes in latency-associated TGF binding protein (LTBP-1) peptide hydrolytic potential. Panel A: Representative examples and Panel B: mean data in FVB wild-type (WT, n = 10 non-PO, 12 PO) versus MT1-MMP over-expression (OE n = 10 non-PO, 9 PO) versus MT1-MMP reduced expression (RE, n = 10 non-PO, 16 PO) mice. MT1-OE mice had an increase in LTBP-1 peptide hydrolysis before and after PO compared with WT mice. By contrast, the MT1-RE mice had a significantly lower LTBP-1 peptide hydrolysis before PO and a significantly blunted increase in LTBP-1 peptide hydrolysis after PO compared with both WT and MT1-OE mice. * = $p < 0.05$ vs. strain matched non PO control, + = $p < 0.05$ vs. conditioned matched FVB WT, # = $p < 0.05$ vs. conditioned matched MT1-OE.

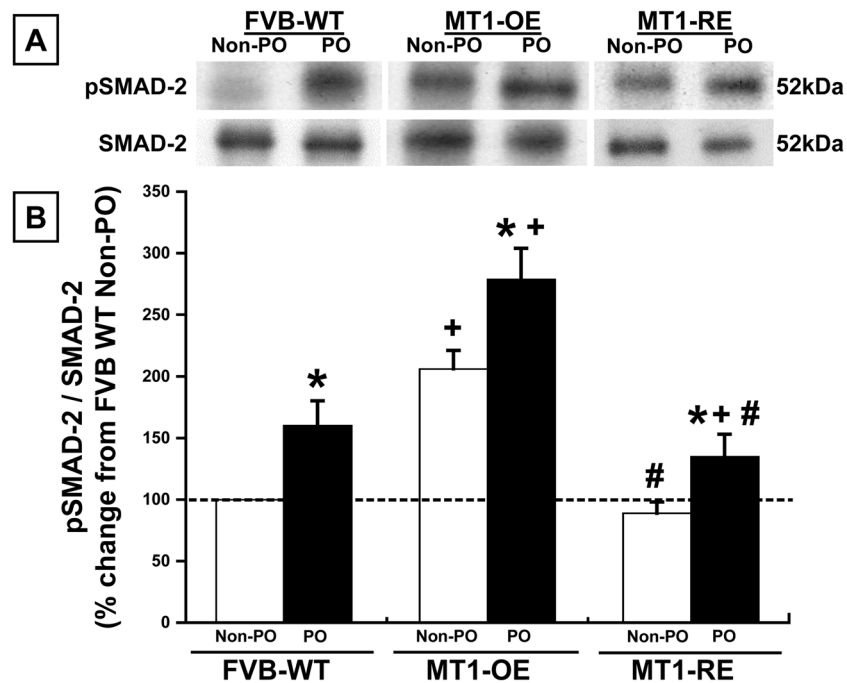


Figure 4. Chronic pressure-overload (PO) induced changes in the pSMAD2/SMAD2 ratio Panel A: Representative examples and Panel B: mean data in FVB wild-type (WT, n = 10 non-PO, 12 PO) versus MT1-MMP over-expression (OE n = 10 non-PO, 9 PO) versus MT1-MMP reduced expression (RE, n = 10 non-PO, 16 PO) mice. MT1-OE mice had an increase in the pSMAD2/SMAD2 ratio before and after PO compared with WT mice. By contrast, the MT1-RE mice had a significantly lower pSMAD2/SMAD2 ratio before PO and a significantly blunted increase in the pSMAD2/SMAD2 ratio after PO compared with both WT and MT1-OE mice. * = $p < 0.05$ vs. strain matched non PO control, + = $p < 0.05$ vs. conditioned matched FVB WT, # = $p < 0.05$ vs. conditioned matched MT1-OE.

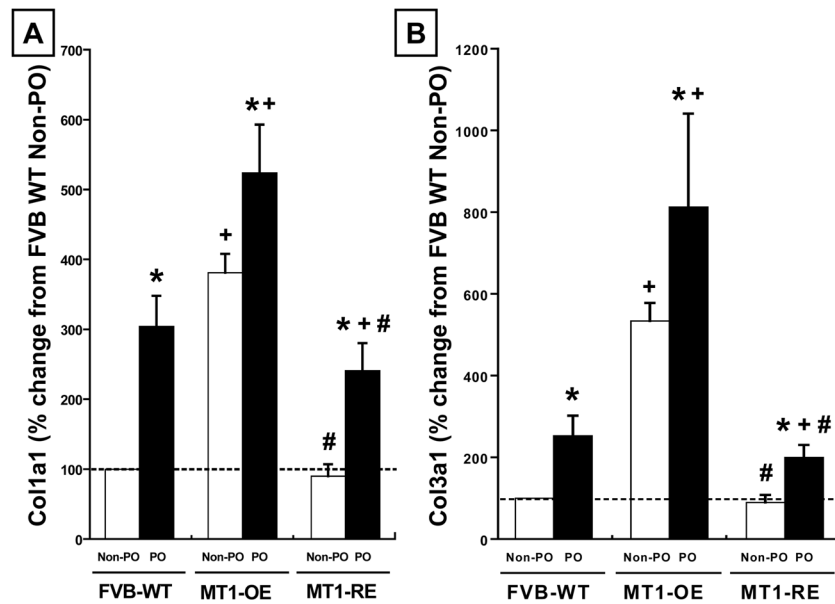


Figure 5.

Chronic pressure-overload (PO) induced changes in collagen 1A1 (Col1A1, Panel A) and collagen 3A1 (Col3A1, Panel B) expression in FVB wild-type (WT, n = 10 non-PO, 12 PO) versus MT1-MMP over-expression (OE n = 10 non-PO, 9 PO) versus MT1-MMP reduced expression (RE, n = 10 non-PO, 16 PO) mice. MT1-MMP OE mice had an increase in Col1A1 and Col3A1 before (non-PO) and after PO compared with WT mice. By contrast, MT1-RE mice had a significantly lower Col1A1 and Col3A1 before PO and a significantly blunted increase in Col1A1 and Col3A1 after PO compared with both WT and MT1-OE mice. * = $p < 0.05$ vs. strain matched non PO control, + = $p < 0.05$ vs. conditioned matched FVB WT, # = $p < 0.05$ vs. conditioned matched MT1-OE.

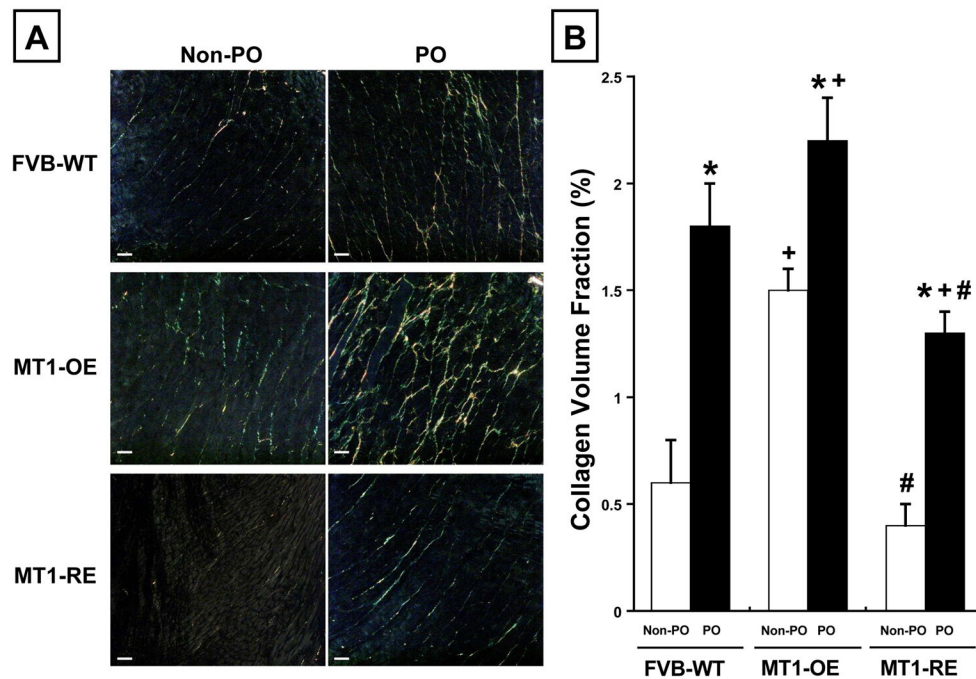


Figure 6. Chronic pressure-overload (PO) induced changes in collagen volume fraction (CVF). Panel A: Representative examples and Panel B: mean data in FVB wild-type (WT, n = 10 non-PO, 12 PO) versus MT1-MMP over-expression (OE n = 10 non-PO, 9 PO) versus MT1-MMP reduced expression (RE, n = 10 non-PO, 16 PO) mice. MT1-MMP OE mice had an increase in CVF before (non-PO) and after PO compared with WT mice. By contrast, MT1-RE mice had a significantly lower CVF before PO and a significantly blunted increase in CVF after PO compared with both WT and MT1-OE mice. * = $p < 0.05$ vs. strain matched non PO control, + = $p < 0.05$ vs. conditioned matched FVB WT, # = $p < 0.05$ vs. conditioned matched MT1-OE.

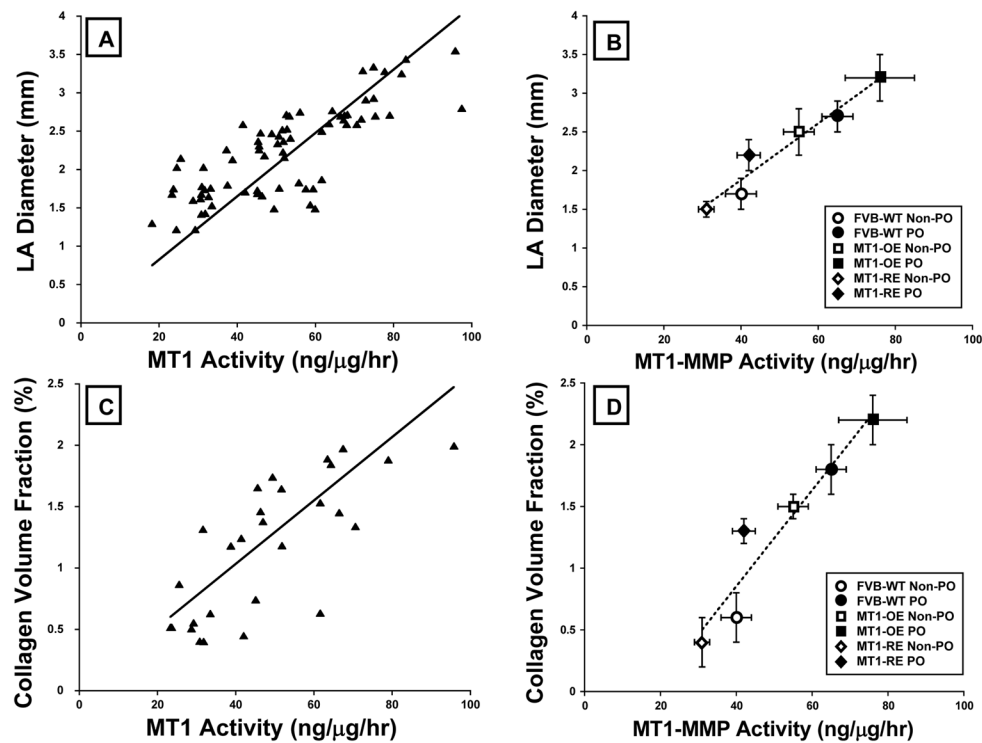


Figure 7. Relationships between membrane type one matrix metalloproteinase (MT1-MMP) and structural, functional and signaling endpoints. There were direct significant relationships between MT1-MMP activity and left atrial diameter (Panel A = individual mice, Panel B = mouse group data), collagen volume fraction (Panel C = individual mice, Panel D = mouse group data). As MT1-MMP increased, left atrial diameter ($r=0.62$, $p<0.001$), collagen volume fraction ($r=0.63$, $p<0.001$). Data from all animals were used to calculate the line of regression (Panels A and C, an data are plotted as mean \pm SEM for each of the 6 groups of mice studied (Panels B and D): FVB wild-type (WT, $n = 10$ non-PO, 12 PO) versus MT1-MMP over-expression (OE $n = 10$ non-PO, 9 PO) versus MT1-MMP reduced expression (RE, $n = 10$ non-PO, 16 PO) mice. PO = mice that underwent transverse aortic constriction induced pressure-overload, non-PO = mice that did not undergo transverse aortic constriction.

Table 1
Effects of PO on structure and function in FVB (wild type) mice and MT1-MMP transgenic mice

	FVB Wild type		MT1-MMP Over expression		MT1-MMP Reduced expression	
	Non-PO	PO	Non-PO	PO	Non-PO	PO
Body Weight (g)	24±1	28±1	28±1	24±1	26±1	28±1
LV Mass (mg)	74±2	132±3*	101±5 ⁺	122±5*	72±2 [#]	129±4*
LV Wall Thickness (mm)	0.8±0.03	1.1±0.03*	0.9±0.02	1.0±0.04*	0.8±0.03	1.1±0.02*
LV Mass / Body Weight (mg/g)	3.0±0.1	4.7±0.1*	3.5±0.1 ⁺	5.2±0.2*	2.8±0.1 [#]	4.6±0.1*
LV Cardiomyocyte CSA (µm ²)	260±10	400±14*	325±21 ⁺	425±20*	250±16 [#]	407±21*
LV End Diastolic Dimension (mm)	3.5±0.1	3.5±0.1	3.7±0.1	4.0±0.2 ⁺⁺	3.5±0.1	3.6±0.1 [#]
LV End Diastolic Volume (µL)	47.9±2.1	47.9±1.5	48.4±1.4	57.1±5.2 ⁺⁺	48.2±1.4	50.7±2.5 [#]
LV Mass / Volume (mg/µL)	1.56±0.05	2.80±0.11*	2.09±0.10 ⁺	2.24±0.17 ⁺⁺	1.71±0.06 [#]	2.61±0.09 ^{##}
LV Fractional Shortening (%)	37±1	33±1*	31±1 ⁺	21±2 ⁺⁺	35±1	33±1 [#]
LV Ejection Fraction (%)	66±1	59±1*	61±2 ⁺	40±3 ⁺⁺	62±2	57±1 [#]
LA Diameter (mm)	1.7±0.2	2.7±0.2*	2.0±0.3 ⁺	3.2±0.3 ⁺⁺	1.5±0.1	2.2±0.2 ^{##}
Sample size (male/female)	10 (5/5)	12 (6/6)	10 (5/5)	9 (6/3)	10 (5/5)	16 (10/6)

MT1-MMP = membrane type 1 matrix metalloproteinase, PO = transverse aortic constriction induced pressure-overload, CSA = cross-sectional area, LA = left atrium, LV = left ventricular, BW = body weight, Values presented as Mean ± SEM,

* p<0.05 vs. strain-matched non-PO

⁺ p<0.05 vs. condition-matched FVB,

[#] p<0.05 vs. condition-matched MT1-MMP over expression.